



národní  
úložiště  
šedé  
literatury

## **Effect of Morphology of Nanostructures to Filter Ultrafine Particles**

Kimmer, D.  
2011

Dostupný z <http://www.nusl.cz/ntk/nusl-161501>

Dílo je chráněno podle autorského zákona č. 121/2000 Sb.

Tento dokument byl stažen z Národního úložiště šedé literatury (NUŠL).

Datum stažení: 19.04.2024

Další dokumenty můžete najít prostřednictvím vyhledávacího rozhraní [nusl.cz](http://www.nusl.cz) .

# Morphology of Nano and Micro Fiber Structures in Ultrafine Particles Filtration

Dusan Kimmer<sup>a</sup>, Ivo Vincent<sup>a</sup>, Jan Fenyk<sup>a</sup>, David Petras<sup>a</sup>,  
Martin Zatloukal<sup>b</sup>, Wannas Sambaer<sup>b</sup> and Vladimir Zdimal<sup>c</sup>

<sup>a</sup>SPUR a.s., T. Bati 299, 764 22 Zlín, Czech Republic

<sup>b</sup>Centre of Polymer Systems, Polymer Centre, Tomas Bata University in Zlín, nám. T.G.Masaryka 5555,  
760 01 Zlín, Czech Republic

<sup>c</sup>Institute of Chemical Process Fundamentals of the AS CR, v.v.i., Rozvojova 135,  
165 02 Praha 6, Czech Republic

**Abstract.** Selected procedures permitting to prepare homogeneous nanofibre structures of the desired morphology by employing a suitable combination of variables during the electrospinning process are presented. A comparison (at the same pressure drop) was made of filtration capabilities of planar polyurethane nanostructures formed exclusively by nanofibres, space polycarbonate nanostructures having bead spacers, structures formed by a combination of polymethyl methacrylate micro- and nanofibres and polypropylene meltblown microstructures, through which ultrafine particles of ammonium sulphate 20 – 400 nm in size were filtered. The structures studied were described using a new digital image analysis technique based on black and white images obtained by scanning electron microscopy. More voluminous structures modified with distance microspheres and having a greater thickness and mass per square area of the material, i.e. structures possessing better mechanical properties, demanded so much in nanostructures, enable preparation of filters having approximately the same free volume fraction as flat nanofibre filters but an increased effective fibre surface area, changed pore size morphology and, consequently, a higher filter quality.

**Keywords:** Morphology optimization, Nanofiber, Beaded nanofiber, Bead defects, Bead formations, Bead spacers, Electrospinning, Nanolayers homogeneity, Filtration efficiency, 3D nanostructure characterization.

**PACS:** 81.16.-c, 81.07.-b, 61.46.-w, 62.25.-g, 62.23.Kn, 62.23.St

## INTRODUCTION

Elimination of ultrafine dust particles, bacteria and viruses from the ambient air and drinking water is becoming increasingly relevant in the present world and is connected with a growing number of respiratory diseases in industrial agglomerations and with a threat of various pandemics.

In order to properly assess the filter quality, it is necessary to consider both the filtration efficiency and the admissible pressure drop ( $\Delta p$ ). It can be assumed that nanofibres will find use primarily in the area of microfiltration (i.e. for removal of particles ranging from 100 nm to 15  $\mu$ m) and ultrafiltration (for particles ranging from 5 nm to 100 nm).

The greatest changes in the nanofibre structures [1] during fibre-forming process in an electrostatic field [2] can be achieved by altering properties of the solution processed (polymer concentration and, consequently, solution viscosity, molar mass of the polymer [3], solution conductivity, polymer permittivity, etc.) and of the process characteristics proper (voltage used, kind and distance of the electrodes, quality and electric conductivity of the collecting substrate, etc.). This work concentrates rather on the effect of co-solvent, various additives and on variations of variables, which do not change the process intensity significantly but allow preparation of nano nonwoven textile (nNT) having high homogeneity, small nanofibre diameter and defined size of globular microspheres in a continuous technological process.

## EXPERIMENTAL

### Materials

PU solution in dimethylformamide (DMF) based on 4,4'-methylenebis(phenylisocyanate) (MDI), poly(3-methyl-1,5-pentanediol)-alt-(adipic, isophthalic acid) (PAIM) and 1,4 butanediol (BD) was synthesized in molar ratio 9:1:8 (PU 918) at 90°C for 5 hours (per partes way of synthesis starting with preparation of prepolymer from MDI and PAIM and followed by addition of BD and remaining quantity of MDI). Density of PU 918  $\rho = 1.1 \text{ g.cm}^{-3}$ . The prepared solutions were suitable for electrospinning and had a PU concentration of 13 wt.%, viscosity of 1.5 Pa.s and conductivity of  $150 \mu\text{S.cm}^{-1}$ . For the preparation of PU mixture the PU 918 was mixed in 1:1 ratio with PU 413 prepared also in DMF from MDI, polyester diol and chain extender in molar ratio 4:1:3.

Used polyamide 6 (PA 6) was Silamid E (Roonamid a.s., Žilina, Slovakia),  $\rho = 1.13 \text{ g.cm}^{-3}$ . PA 6 solutions in acetic and/or formic acid were prepared always in concentration of 8 wt.%.

Tested polycarbonate (PC) was Macrolon 2458 (Bayer, Leverkusen, Germany) had a density  $\rho = 1.2 \text{ g.cm}^{-3}$ . PC solution for electrospinning was prepared in mixture of solvents tetrachlorethane : chloroform = 3:1 and adjusted by ionic liquids 1-ethyl-3-methylimidazolium-bis(trifluoromethylsulfonyl)imide : 1-ethyl-3-methylimidazolium triflate = 2:1 (IoLiTec Ionic Liquids Technologies, Heilbronn, Germany) and 1 wt.% of Borax. 12.5 wt.% PC solution had a viscosity of 0.3 Pa.s and conductivity  $10.5 \mu\text{S.cm}^{-1}$ .

Used Polymethylmethacrylate (PMMA) was Altuglas V 046 (Altuglas International, La Garenne-Colombes cedex, France) with density  $\rho = 1.18 \text{ g.cm}^{-3}$ . PMMA solution in DMF : toluene = 1:1 used for electrospinning had a concentration of 20 wt.%, viscosity of 0.11 Pa.s and conductivity of  $1.3 \mu\text{S.cm}^{-1}$ .

### Filter Sample Preparation by Electrospinning Process

Nanofiber layers were prepared from polymeric solutions with a commercially available NanoSpider<sup>TM</sup> machine (Elmarco s.r.o. Liberec, Czech Republic, <http://www.elmarco.com/>) equipped with patented rotating electrode with 3 cotton

cords spinning elements (PCT/CZ2010/000042) or set of nanofibers forming jets. The experimental conditions were as follows: relative humidity 25 - 36%, temperature 22°C, electric voltage applied into PU solution 35 through 75 kV, distance between electrodes 210 mm, rotational electrode speed 7 rpm and speed of supporting textile collecting nanofibers was 0.16 – 0.32 m.min<sup>-1</sup>. Nanofibres were collected on polypropylene (PP) or viscose nonwoven textiles (NT).

### **Filter Sample Characterization**

Nanofiber based filter, prepared through the electrospinning process, has been characterized by the Scanning Electron Microscope (SEM, Vega 3, Tescan, Czech Republic). The obtained SEM pictures have consequently been used for the determination of fibre diameter, nanofibre layer thickness and fibre diameter/pore size distribution by using recently proposed digital image analysis technique [4-6].

In order to properly describe the overall performance of a filtration material, we used the quality factor defined as  $qF = \ln(1/P)/\Delta p$  where  $P$  is the filter penetration and  $\Delta p$  is the pressure drop [7].

### **Filtration Efficiency Measurement**

All manufactured nanofibre based filtration materials were measured for aerosol (di-ethyl-hexyl-sebacate with geometrical average of particle diameters 0.45 µm) penetration at constant air flow rate 30 l.min<sup>-1</sup>. (face velocity 5.7 cm.s<sup>-1</sup>) by means of filter measuring system LORENZ (Germany) adjusted for EN 143.

In the ultrafine particle size range, the filtration efficiency was determined as a function of particle diameter (results presented on Figures 17 and 18). The 1 g.l<sup>-1</sup> ammonium sulphate solution was nebulized (AGK, PALAS, Germany), a monodisperse size fraction was selected using an Electrostatic Classifier (EC 3080, TSI, USA), and particle concentration upstream and downstream the filter (face velocity 5.7 cm.s<sup>-1</sup>) was recorded by a condensation particle counter (UCPC 3025 A, TSI, USA). The filtration efficiency was determined at nine mobility diameter fractions: 20, 35, 50, 70, 100, 140, 200, 280 and 400 nm.

## **RESULTS AND DISCUSSION**

### **1. EFFECT OF SELECTED VARIABLES ON ELECTROSPINNING PROCESS, NANOFIBRE DIAMETER AND STRUCTURE OF NANOLAYERS FORMED**

The most important requirement for quality of nNT with respect to their use in filtration products are **homogeneity** of the layer, nanofibres **space layout** and preparation of nanofibres having the smallest possible **diameter** as shown by the 2D and 3D preceding modelling of particle collection efficiency [8, 9].

While optimising the structure of the nanofibre layers it is absolutely essential to monitor many variables connected with the solution adjustment (polyurethane synthesis) [3], properties and composition of the solutions prepared and the electrospinning process proper.

## 1.1 Effect of Selected Electrospinning Variables on Nanostructure Homogeneity

### 1.1.1 Nanofibre Structure Defects Produced During Electrospinning

The most frequent complication worsening service properties of nNT is the formation of holes, which occurs usually in case of low intensity of electrospinning process (Figure 1) or in case of excessively diluted solutions due to impact of solution drops on nNT (Figure 2).

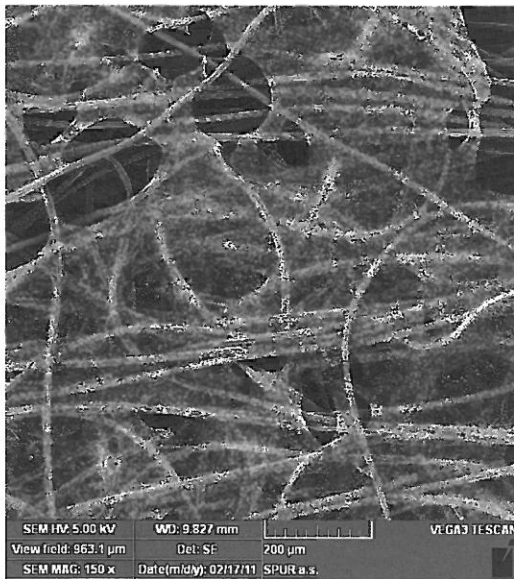


**FIGURE 1.** Holes in a PU nanolayer at low process intensity, magnification 150×.

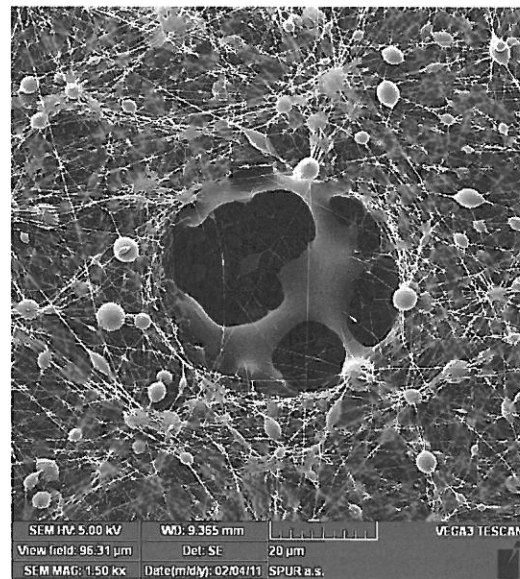


**FIGURE 2.** Holes in a PU nanolayer caused by fall of solution droplet on formed nanostructure, magnification 1 500×.

Another frequent defect is the accumulation of the nanofibres around conductive microfibrils of the collecting substrate (Figure 3) that can be eliminated by optimizing the electrospinning process (Figure 4). Combinations of almost 20 parameters were used to prepare PU nanolayers with requested homogeneity (Figure 4). Among them solution conductivity, collecting substrate, used spinning electrode and applied voltage were the most important.



**FIGURE 3.** Accumulation of PU nanofibres around conductive microfibres of a spunbond support, magnification 500×.

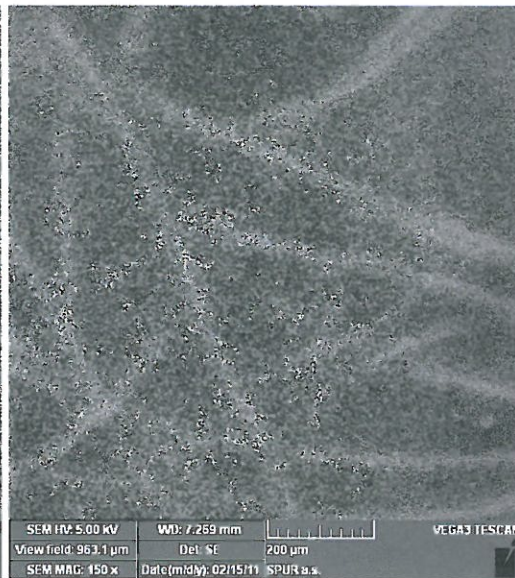


**FIGURE 4.** Homogenous lay-out of PU nanofibres around microfibres of a spunbond support, magnification 150×.

### 1.1.2 Influence of Spinning Electrode Design

Figure 5 shows the spinning cones formed on the surface of non-conducting spinning elements (PCT/2010/000042) prepared from threads or textile cords, that influence positively the homogeneity of nanolayer deposition.

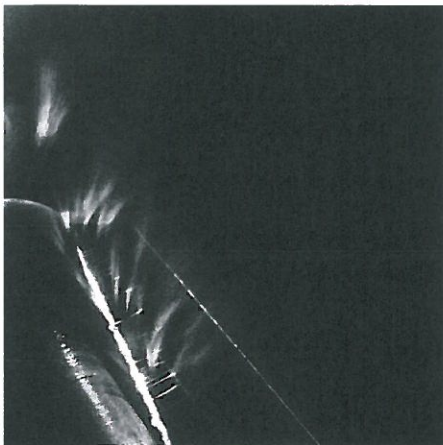


**FIGURE 5.** Detail of Taylor cones formed on cord spinning elements.

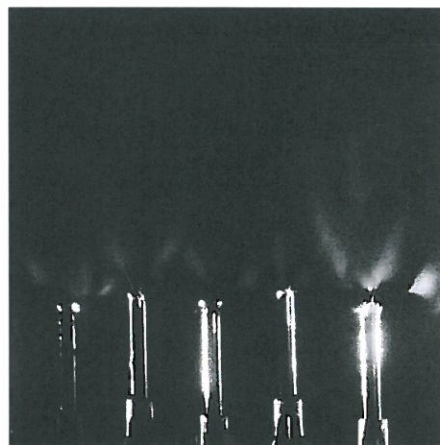


**FIGURE 6.** Detail of Taylor cones formed on jet electrodes.

At this arrangement of the electrostatic process the electric field alone controls frequency and shape of the Taylor cones. By using thread electrodes the diameter of the nanofibres being formed can also be decreased significantly. We managed to achieve a formation of numerous primary jets on the fibre-forming electrode leading to formation of homogeneous nanostructures even on jet electrodes (Figure 6).

## 1.2 Preparation of Homogenous nNT Comprising Small-Diameter Nanofibres

### 1.2.1 Influence of Solvent and Solution Conductivity

Influence of solvent and relative humidity on fibre diameter formed was described in our previous works [8, 9]. In the following images (Figures 7 and 8), a comparison is made of two nanostructures prepared from PA 6 dissolved *i)* in a blend of solvents  $\text{CH}_3\text{COOH} : \text{HCOOH} = 2:1$  (electric conductivity of the solution prepared in this manner  $\chi \sim 198 \mu\text{S}\cdot\text{cm}^{-1}$ ) and *ii)* in  $\text{HCOOH}$  alone, the use of which results in a marked increase of electric conductivity to  $\chi \sim 4,150 \mu\text{S}\cdot\text{cm}^{-1}$ . The mass per square area of both samples under comparison is  $AM \sim 0.42 \text{ g}\cdot\text{m}^{-2}$ .

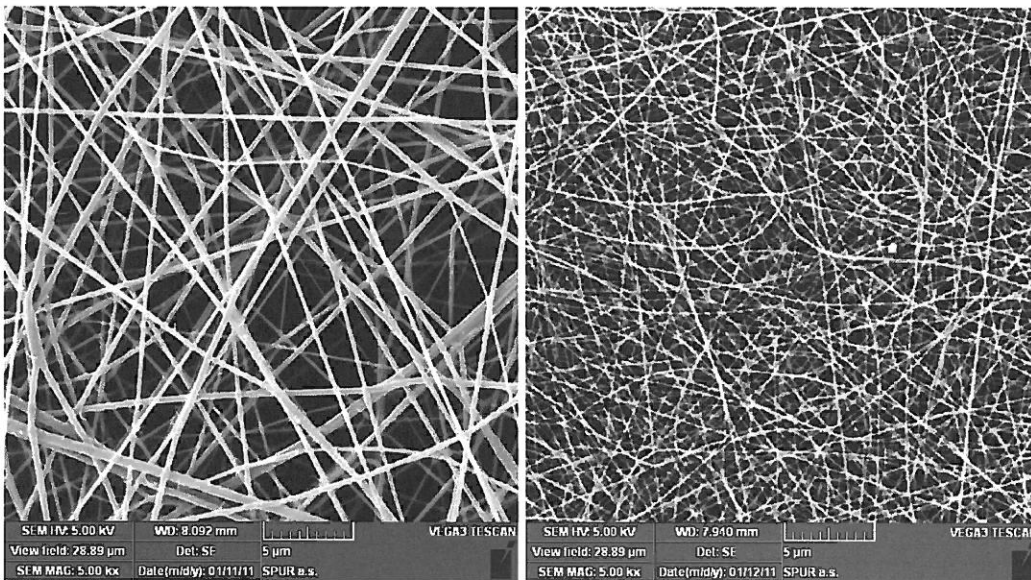


**FIGURE 7.** PA 6 nanofibres prepared from mixture of  $\text{CH}_3\text{COOH}$  and  $\text{HCOOH}$  (2:1), magnification 5 000 $\times$ ,  $d_f = 228 \text{ nm}$ .

**FIGURE 8.** PA 6 nanofibres prepared from  $\text{HCOOH}$  only, magnification 5 000 $\times$ ,  $d_f = 1 \text{ nm}$ .

Nanofibre diameter affects positively filtration efficiency of nNT but markedly increases the pressure drop, primarily in case of flat structures. Therefore, we concentrated on the study of filtration properties of space structures having as greatest volume and as smallest pore sizes as possible in an attempt to prepare materials possessing a high filtration performance – low pressure drop at high filtration efficiency, i.e. high quality factor.

## 2. CONTROLLED PREPARATION OF NANOSTRUCTURES WITH REQUESTED MORPHOLOGY

### 2.1 Elimination of Bead Defects in Nanostructure

During the electrospinning process, we always monitor the whole set of variables and never change more than one variable in comparison experiments. By utilising a modification additive (Borax and/or citric acid) for conductivity improvement of the PU solution spinned (15 mass percent in DMF) a marked elimination of bead defects can be achieved (Figures 9 and 10).

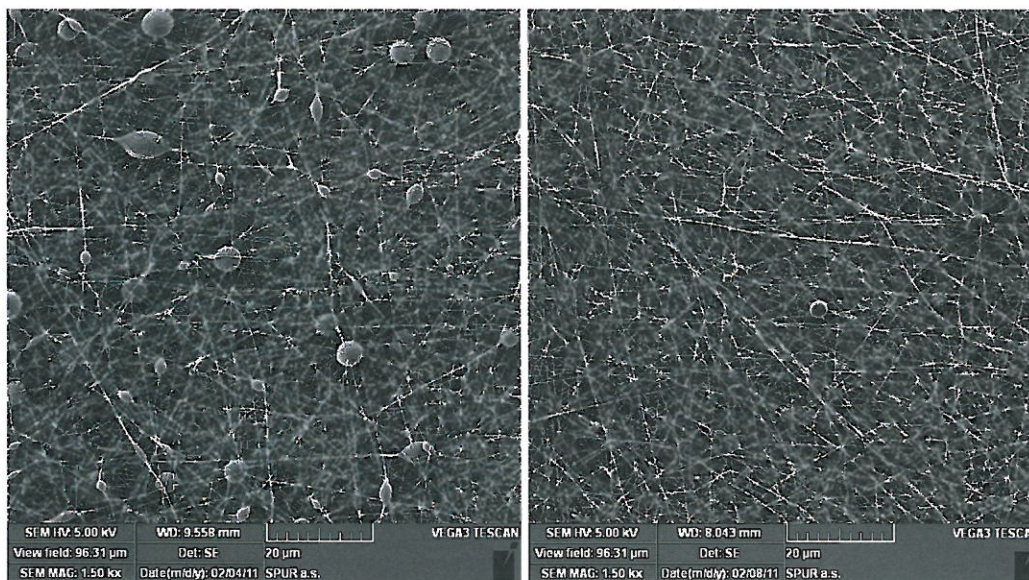


**FIGURE 9.** Nanostructure formed without any additives, magnification 1 500×.

**FIGURE 10.** Nanostructure formed in presence of  $\text{Na}_2\text{B}_4\text{O}_7 \cdot 10 \text{H}_2\text{O}$  and citric acid, magnification 1 500×.

Presence of the bead defect in PU structures can be eliminated very efficiently also by addition of surface active agents, for instance ionic liquids (Figures 11 and 12). A change was achieved by the addition of 1 mass percent (related to the polymer dry matter) of 1-ethyl-3-methylimidazolium bis(trifluoromethylsulfonyl)imide supplied by IoLiTec Ionic Liquids Technologies, Germany.



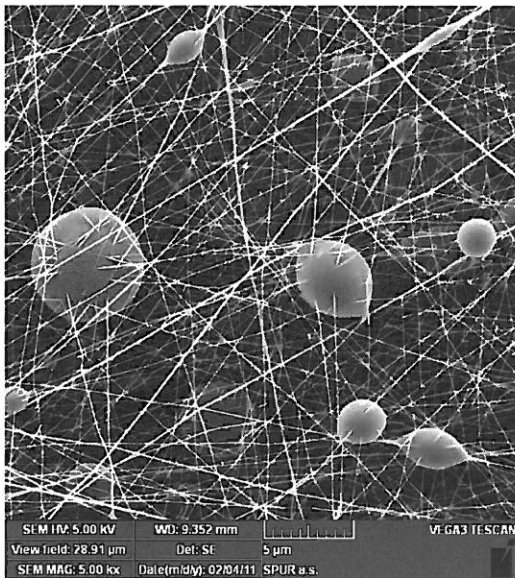


**FIGURE 11.** Nanostructure formed without any additives, magnification 5 000×.

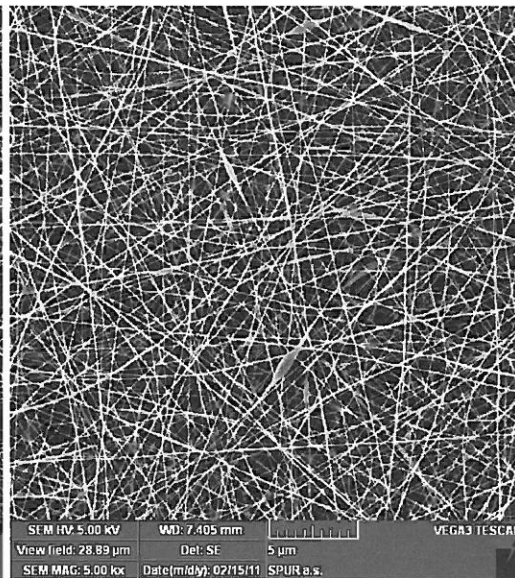


**FIGURE 12.** Nanostructure formed in presence of ionic liquid, magnification 5 000×.

On the contrary, a regular distribution of bead formations in the nanostructure results in a physical separation of the nanofibre layers and it will be interesting to examine the effect on the filtration performance of such nanostructures.

## 2.2 Controlled Formation of Beads Nanostructures with Organized and Random Space Layouts

### 2.2.1 Polycarbonate Space Organized Nanostructures Containing Bead Formations

Based on the dependences revealed, an increase in the content of nanofibres among beads and formation of a regular structure with bead spacers cumulated in columns interlinked with nanofibres were achieved in the preparation of polycarbonate nanostructures by changing the solvent system (by the addition of chloroform to tetrachlorethane) and by adding Borax (Figures 13 and 14). Such a morphology, similar to honeycombs, leads to an increase in thickness and mass per square area of the filtration material and positively influences the filtration properties as discussed below.

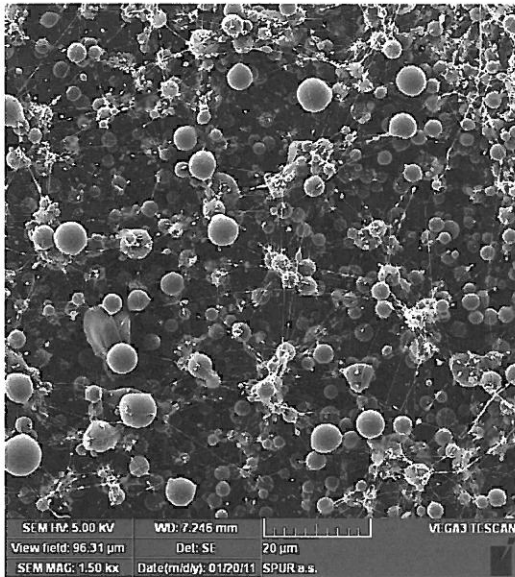


**FIGURE 13.** Structure of PC before the optimisation process, magnification 1 500×.

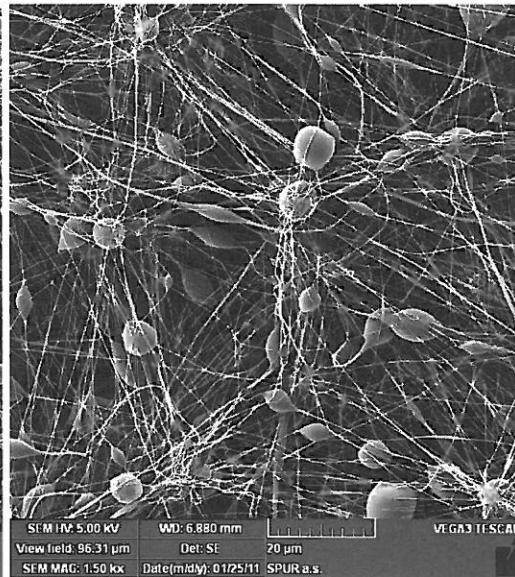


**FIGURE 14.** Nanostructure of PC after the optimisation process, magnification 1 500×.

Particles penetration through this structure with organized space layout (Figure 14) having mass per square area of  $3.42 \text{ g.m}^{-2}$  was 0.762% at the pressure drop of 35 Pa, which corresponds to  $qF = 139$  (measured on Lorenz instrument according to EN 143 standard).

### 2.2.2 Space Nanostructures from PU Blends

With respect to brittleness of the nanostructures prepared from PC an attempt was made to prepare space nanostructures also from high elasticity PU. Blends of PU solutions having various molar mass distributions were combined where at given electrospinning conditions, one forms fine fibres and the other rather spheres or bead formations. By varying parameters of the electrostatic process, materials with a random (Figure 15) as well as organized distributions of defects were prepared. When their filtrating performance was examined, these materials exhibited lower pressure drops than nanostructures without bead formations at identical filtration efficiency.

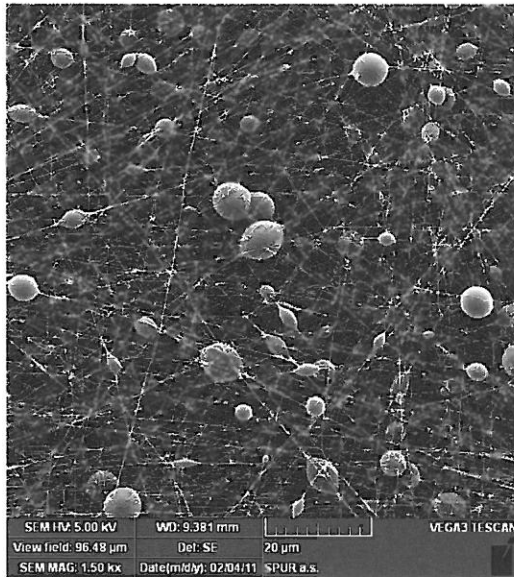


**FIGURE 15.** Random nanostructure of PU mixture without addition of surface tension agent, magnification 1 500×.

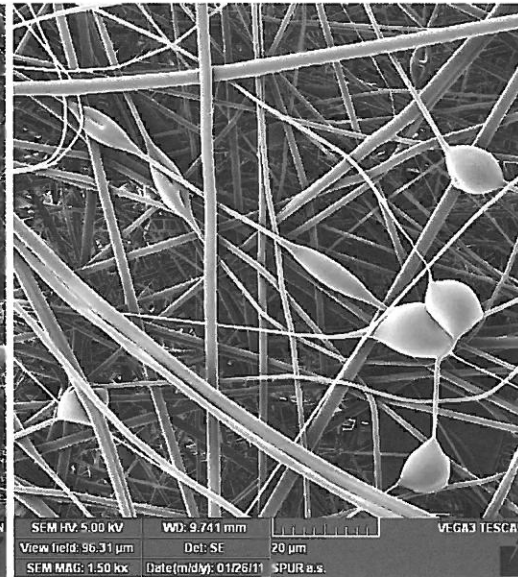


**FIGURE 16.** PMMA structure comprising fibres with a broad distribution and bead defects, magnification 1 500×.

### 2.3 Structures Prepared from Fibres with a Broad Distribution of Fibre Diameters and Bead Formations

An increase in thickness of the fibrous structure was achieved in the PMMA structure by combining bead spacers with nano- and microfibrils (Figure 16). According to our experience also this combination of globular and microfibril spacers leads to an improvement of filtration properties of the material.

## 3. FILTRATION PERFORMANCE AND 3D CHARACTERIZATION OF FIBROUS STRUCTURES

Filtration properties and dimensional characteristics of flat PU (Figures 10 and 12) and space PC (Figure 14) nanostructures are summed up in Table 1. In order to be able to compare effect of the structure on filtration efficiency we always compare structures having the same pressure drop of ~ 90 Pa.

TABLE 1. Characterisation and properties of space and flat nanostructures.

Structures with pressure drop ~ 90 Pa				
Sample	Nanostructure with arranged space layout PC 86	Nanostructure of PU with flat layout PU 110	Nanostructure of PU with flat layout PU 90	Nanostructure of PU with flat layout PU 89
Area mass ( $\text{g}\cdot\text{m}^{-2}$ )	6.800	0.447	0.807	0.438
Thickness ( $\mu\text{m}$ )	30.2*	2.6*	9.2*	3.5*
SVF ( $\text{m}^3\cdot\text{m}^{-3}$ )	0.188	0.156	0.080	0.113
Filtration properties measured by Lorenz adjusted for EN 143				
Pressure drop (Pa)	78	93 -100	117 - 137	121 - 124
Filtration efficiency (%)	99.880	99.860 – 99.900	99.946–99.970	99.609 – 99.832
Quality factor ( $\text{kPa}^{-1}$ )	86	68 - 73	54 - 64	45 - 53
Filtration properties measured as function of particle size				
MPPS (nm)	100	70	70	70
Pressure drop (Pa)	81 - 95	110	90	89
Filtration efficiency at MPPS (%)	98.900	90.962	90.350	88.425
Quality factor at MPPS ( $\text{kPa}^{-1}$ )	51	22	26	24
Results based on digital image analysis of SEM images				
Average fiber diameter (nm)	120.2	107.2	124.7	113.0
Pore size distribution (nm)	$D_n$ 202.5 $D_w$ 740.0 $D_z$ 1,269.0 $D_{z+1}$ 1,721.0	201.0 376.0 553.0 728.0	139.0 327.0 493.0 640.0	99.0 293.0 453.0 597.0
Effective surface area in filter ( $\text{m}^2\cdot\text{m}^{-2}$ )	188.9	15.1	23.6	14.0

\* Measured from SEM pictures.

Neither variations of mass per area ( $0.44 - 0.81 \text{ g}\cdot\text{m}^{-2}$ ) nor those of fibre diameters (107 - 125 nm) in flat PU nanostructures lead to such an increase in the filtration efficiency that can be obtained with the space nanostructure (Table 1, Figure 14).

While effective surface area in flat PU nanostructures does not change, it increases dramatically in PC space nanostructure (Figure 14) but the solid volume fraction (SVF) and consequently free volume fraction of compared space and flat nanostructures do not change too much. With respect to the fact that the dominant mechanism operating in collection of ultrafine particles is diffusion, it can be assumed that in the case of space structure the probability of particle collection on the surface of nanofibres or on the surface of bead formation will increase due to longer path of the ultrafine particle performing Brownian motion.

The structures characterized in Table 2 show approximately half of the pressure drop occurring in formations given in Table 1. We concentrate intentionally on low pressure drops with respect to a potential application of nanostructures in face half-masks and in mask filters. The microstructure from PP meltblown material, which, in addition, exhibits a mechanism of antistatic capture, is compared with

nanostructure from PU nanofibres and a combined structure prepared from a blend of PMMA nanofibres and microfibrils, that act like spacers increasing thickness and volume.

**TABLE 2.** Characterisation and properties of flat nanostructure, microstructure and combined micro- and nanofiber structure.

<b>Structures with pressure drop ~ 45 Pa</b>			
<b>Sample</b>	<b>Combined structure of PMMA with space layout</b>	<b>Nanostructure of PU with flat layout</b>	<b>Microstructure of PP</b>
Area mass (g.m <sup>-2</sup> )	6.920	0.403	54.780
Thickness (μm)	34.7		440.0**
SVF (m <sup>3</sup> .m <sup>-3</sup> )	0.169	0.080	0.138
<b>Filtration properties measured by Lorenz adjusted for EN 143</b>			
Pressure drop (Pa)	25	68	28
Filtration efficiency (%)	98.905	99.564	98.117
Quality factor (kPa <sup>-1</sup> )	181	80	142
<b>Filtration properties measured as function of particle size</b>			
MPPS (nm)	50	100	50
Pressure drop (Pa)	48	35	60
Filtration efficiency at MPPS (%)	97.52	78.77	91.67
Quality factor at MPPS (kPa <sup>-1</sup> )	77	44	41
<b>Results based on digital image analysis of SEM images</b>			
Average fiber diameter (nm)	758.6	124.7	831.8
Pore size distribution (nm)	$D_n$	672.0	139.0
	$D_w$	2,564.0	327.0
	$D_z$	4,409.0	493.0
	$D_{z+1}$	6,151.0	640.0
Effective surface area in filter (m <sup>2</sup> .m <sup>-2</sup> )	30.9	11.8	292.0

\* Measured from SEM pictures.

\*\* Measured by thickness gauge SOMET (Hradec Králové, Czech Republic).

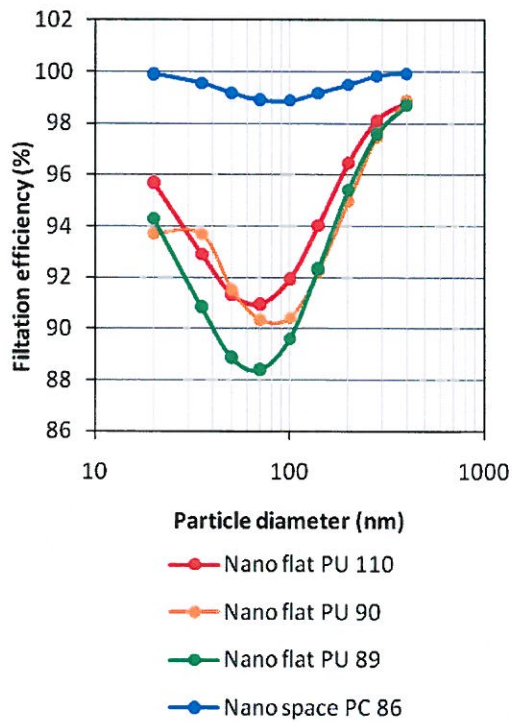


**FIGURE 17.** Filtration efficiency of flat and space organized nanostructures. Pressure drop of all materials ~ 90 Pa.

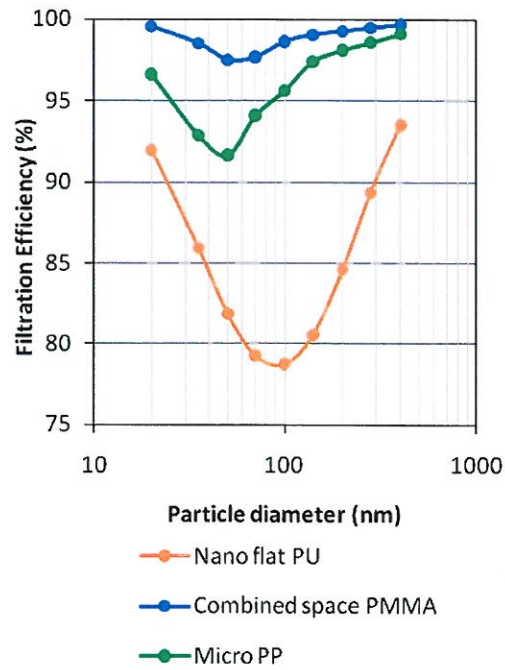


**FIGURE 18.** A comparison of planar nanostructure with microfibre structure and a structure formed by a combination of nano- and microfibres. Pressure drop of compared materials ~ 45 Pa.

Materials having various morphology of fibre arrangement (Tables 1 and 2) were analysed with respect to their space layout and capability to capture ultrafine particles (Figures 17 and 18). More voluminous (more bulky) structures containing nanofibres and distance microspheres are more efficient in the area of capture of ultrafine particles at identical pressure drop of materials.

In order to establish a mechanism of improvement of the filtration capability in voluminous (bulky) structures we searched for a reply to a question how pore sizes and their distribution change in studied structures. For this assessment carried out on actual nanofibre structures produced we used recently proposed digital analysis of SEM images [4-6]. The analysis was based on an examination of the change in richness of grey halftones caused by a change in the thickness of nanofibre nonwoven textiles. In more detail, all nanostructure pores were loaded with fractions of model spheres to identify pore size distribution.

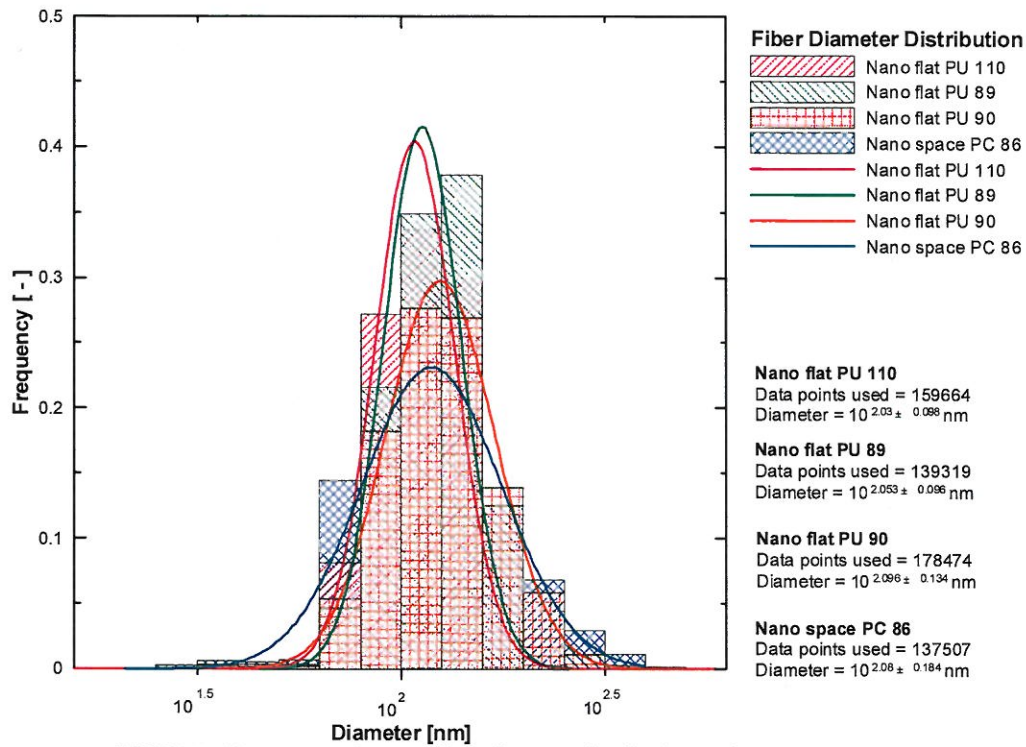


FIGURE 19. A comparison of fibre diameter distribution in filters from Table 1.

In Figures 19 and 21, fibre diameter distributions in the structures tested are summed up. The bars show the measured values, whereas the line is the distribution function based on Gaussian distribution approximation.

From the comparison of pore size distributions in the nanostructures prepared (Figure 20) it is apparent that pore size distributions in case of the space layout of the nanostructure with bead spacers has broader pore size distribution, contains more voluminous pores but the average value pore size distributions do not differ very much from flat nanostructures when materials having as much as 15 times greater mass per square area and 11 times greater thickness were compared. Space layout of nanostructure increases physical separation of nanofibre layers and distances between individual nanofibres and changes nanofibre deposition angles. Such a structure morphology is the reason of filtration performance improvement.

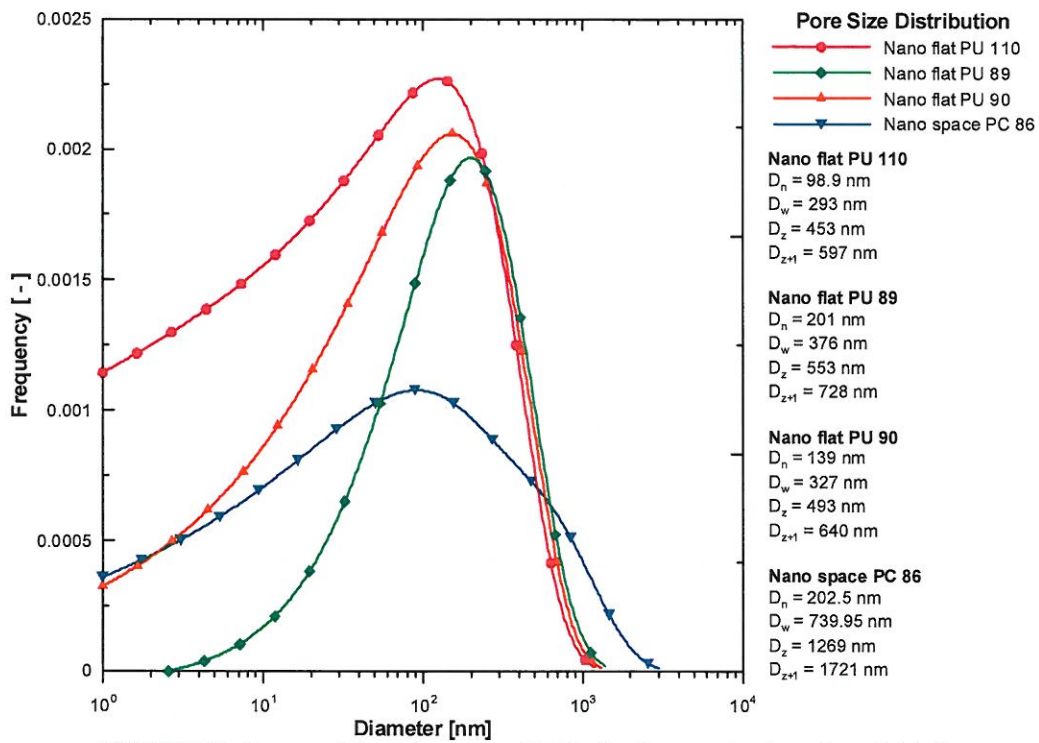


FIGURE 20. A comparison of pore size distribution in nanostructures from Table 1.

A comparison of structures containing microfibres (Figures 21 and 22) shows a positive effect of the presence of nanofibres (Figure 16) on filtration efficiency. Polypropylene (PP) melt blown microstructure and a combined PMMA structure have approximately the same average fibre diameter (Figure 21) but differ by fibre distributions (nanofibre content) and pore size distributions (Figure 22). In addition, the PP melt blown material exhibited a pressure drop of 60 Pa, which means that at the 45 Pa required, its filtration efficiency would be somewhat worse than presented in Figure 18. For comparison, also properties achieved with the flat PU nanostructure are presented in Figures 18, 21 and 22.



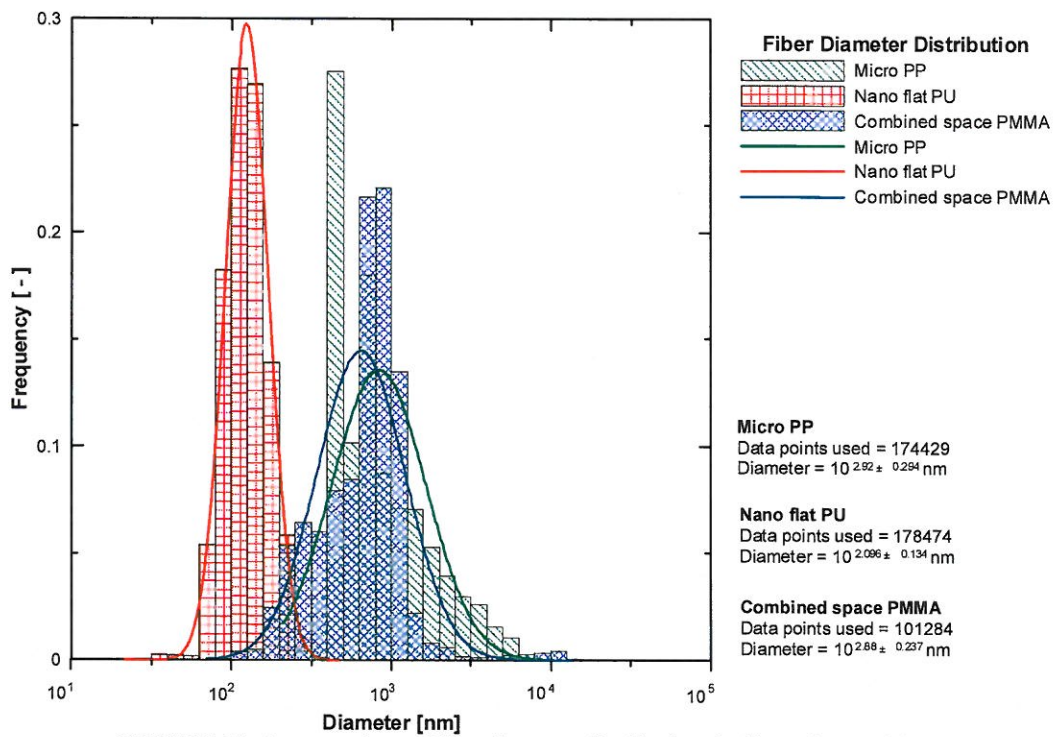


FIGURE 21. A comparison of fibre diameter distributions in filters from Table 2.

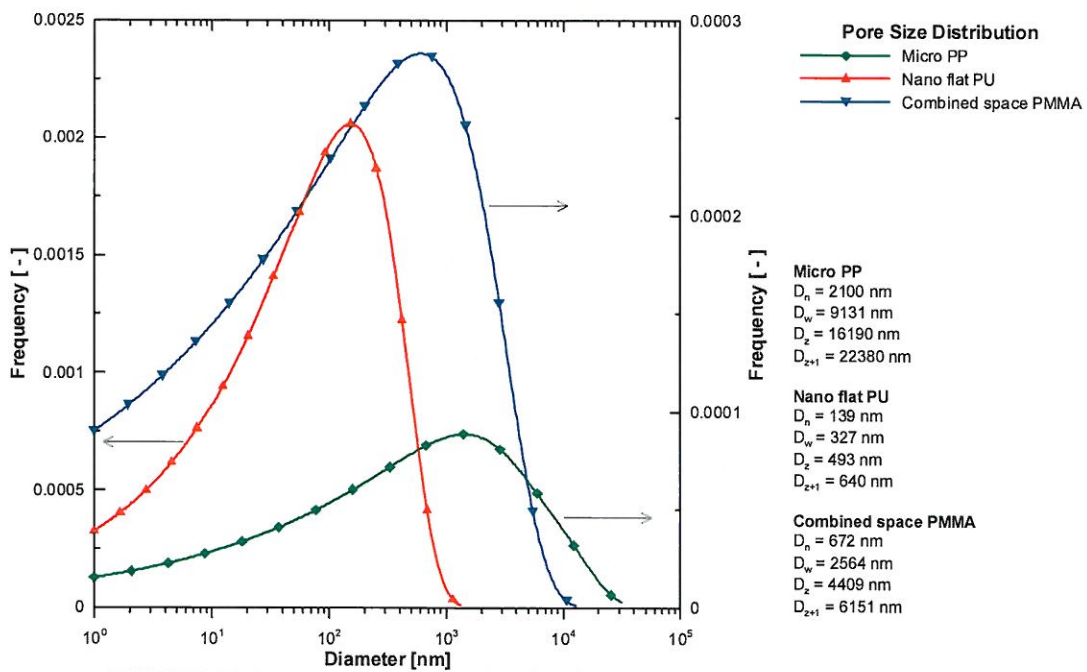


FIGURE 22. A comparison of pore size distributions in the structures from Table 2.

## CONCLUSIONS

The work presents electrospinning procedures that permit to obtain flat nanostructures, space nanostructures with bead microspheres and structures having a broad distribution of fibres. An incorporation of bead spacers into the nanofibre structures results in an increase of thickness and mass per square area of the material. It has a positive effect on its mechanical properties, increase in distances between nanofibres, increase of active surface for particle capture due to an increase of solid volume fraction, with no marked change in free volume fraction in comparison with the flat nanofibre structure. These facts then positively affect filtration performance when ultrafine particles are separated. Using digital analysis of SEM images an effect of structural changes on an increase in filtration properties was confirmed and a positive influence of nanofibre presence in filtrating structures was proved.

The results presented show a way how to further increase the filtration performance of nanofibre filtration textiles.

## ACKNOWLEDGMENTS

This work has been supported by the grant of Czech Ministry of Industry and Trade Nos. 2A-1TP1/068 and FR-TI1/053.

## REFERENCES

1. D. Kimmer, P. Slobodian, D. Petras, M. Zatloukal, R. Olejnik and P. Sáha, *J. of App. Polym. Sci.* **111**, 2711-2714 (2009).
2. S. Ramakrishna, F. Kazutoshi, W. E. Teo, T. C. Lim and Z. Ma, *An Introduction to Electrospinning and Nanofibers*, Singapore: World Scientific Publishing Co. Pte. Ltd., 2005.
3. D. Kimmer, M. Zatloukal, D. Petras, I. Vincent and P. Slobodian, *AIP Conference Proceedings* **1152**, 305-311 (2009).
4. W. Sambaer, M. Zatloukal and D. Kimmer, *AIP Conference Proceedings* **1152**, 312-322 (2009).
5. W. Sambaer, M. Zatloukal and D. Kimmer, *Polymer Testing* **29**, 82-94 (2010).
6. W. Sambaer, M. Zatloukal and D. Kimmer, *Chem. Eng. Sci.* **66**, 613-623 (2011).
7. W. C. Hinds, *Aerosol Technology: Properties, Behavior, and Measurement of Airborne Particles*. 2<sup>nd</sup> Ed., New York: Wiley, 1999.
8. D. Kimmer, I. Vincent, D. Petras, M. Zatloukal, W. Sambaer, H. Salmela and M. Lehtimäki, Application of nanofibres in filtration processes, In: European Conference on Fluid-Particle Separation, October 5th - 7th, 2010, Lyon France.
9. D. Kimmer, I. Vincent, D. Petras, M. Zatloukal, W. Sambaer, P. Slobodian, H. Salmela, M. Lehtimäki and V. Zdímal, "Application of nanofibres in filtration processes" 2<sup>nd</sup> Nanocon International conference, Oct 12-14, 2010, Olomouc, Czech Republic, pp. 415-422.